Use of LCD Panel for Calibrating Structured-Light-Based Range Sensing System

Zhan Song and Ronald Chung, *Senior Member, IEEE*

***Abstract*—Calibration is a crucial step in structured-light-based range sensing device. The step involves the determination of the intrinsic parameters of both the camera and the projector that constitute the device and the extrinsic parameters between the two instruments. The traditional solution requires the use of an external calibration object with an accurately measured pattern printed on it. This paper presents a calibration design that makes use of a liquid-crystal display (LCD) panel as the calibration object. The LCD panel's planarity is of industrial grade and is thus dependable. The pattern shown on the LCD panel is programmable and is thus convenient to produce in high precision. We show that, with the design, the projector-and-camera system parameters can be calibrated with far fewer images with much higher accuracy. Extensive experiments are shown to illustrate the dramatic improvement in performance.**

***Index Terms*—Calibration, liquid-crystal display (LCD) panel, projector-and-camera system, structured light system.**

I. Introduction

THE STRUCTURED-LIGHT-Based System (SLS) is one of the more convenient and accurate visual methods for 3-D reconstruction [1]. It is convenient, because it requires only one camera and a projector to operate and needs no dense texture in the target surface to determine depth. It is accurate, because it determines depth by the optical triangulation mechanism and generally can achieve higher accuracy in depth determination than other visual methods, such as Shape from Shading [2] and Shape from Focus or Defocus [3]. The essence of SLS is that it allows the correspondence task, which is a prerequisite of the triangulation mechanism, to be much simplified by introducing unique coding to every feature point of the projected pattern. The coding scheme could be Gray code [4], Phaseshift [5], M-array [6], or others. If subpixel techniques [7] are used in processing the image data, accuracy in 3-D reconstruction can be enhanced even further.

Calibration is, however, a crucial step in SLS. Both the camera and the projector are required to be accurately calibrated for accurate depth recovery. Traditional calibration comprises two stages: 1) camera calibration and 2) projector calibration. Camera calibration has widely been researched. As for projector calibration, there is an important difference from camera calibration. Since the projector cannot actually image the scene, methods for camera calibration cannot directly be adopted. The traditional calibration setting requires the use of a carefully constructed calibration object whose dimensions are precisely known or measured. One of the often-used calibration objects is a planar surface with an accurately measured pattern printed on it. The calibration plane can be rotated and freely translated in the visual field of the camera, and it is imaged by the camera. From the image data of the pattern print on the calibration plane, the camera's intrinsic parameters, as well as its position and orientation with respect to the calibration object, can be determined. In the second stage, the calibrated information of the camera is used for projector calibration. With the spatial position of the calibration plane unchanged, a known pattern is projected from the projector onto the calibration plane whose reflection is imaged by the camera. The image information allows feature correspondences between the image plane of the camera and the image plane of the projector (we refer to the pattern generation panel of the projector as the image plane of the projector) to be drawn and, in turn, allows the projector's intrinsic parameters, as well as its position and orientation with respect to the calibration plane, to also be determined. Using the calibration object as the bridge between the camera end and the projector end, the positions of the camera and projector can be related, and their relative geometry can be determined.

Obviously, calibration errors in the camera will be propagated to projector calibration and enlarged there. Our experiments show that projector calibration could have an error that is one order of magnitude larger than that of camera calibration. Hence, the accuracy of camera calibration determines the whole system's performance. To improve calibration accuracy, elaborate patterns need to be used. In many of the existing systems, these patterns are produced with precision as fine as 0.1 mm, and they are usually specially designed. This leads to inconvenience and high cost. On the other hand, if the widely adopted less-costly version of the calibration object—a pattern print glued onto a planar surface to form a calibration plane—is used, other problems arise. The pattern print has limited accuracy in its metric figures. The planar surface has uncertain planarity. There is also the inevitable folding of the print against the planar surface, leading to further compromise in the planarity of the calibration plane. All these would limit the calibration accuracy.

In this paper, we present a calibration design that makes use of a liquid-crystal display (LCD) panel as the calibration plane. Whereas patterns displayed on it are used for camera calibration, patterns projected onto and reflected by it when it

Manuscript received May 30, 2007; revised January 24, 2008. The work was supported in part by the Research Grants Council of the Hong Kong Special Administrative Region, China, under Project CUHK4195/04E.

The authors are with the Department of Mechanical and Automation Engineering, The Chinese University of Hong Kong, Hong Kong, China (e-mail: zsong@mae.cuhk.edu.hk; rchung@mae.cuhk.edu.hk).

Color versions of one or more of the figures in this paper are available online at http://ieeexplore.ieee.org.

Digital Object Identifier 10.1109/TIM.2008.925016

is set to total dark are used for projector calibration. The LCD panel's planarity is of industrial grade and is thus far more dependable; even consumer-level LCD panels have the assurance that the substrate glass surface of the panel has a planarity deviation of no more than 0.05 μm [16]. The pattern shown on the LCD panel is programmable and is thus convenient to produce in high precision. We show that, with the design, the projector-and-camera system parameters can be calibrated with far fewer images and much higher accuracy. All in all, the whole system can be built from off-the-shelf, low-cost components, is convenient to use, and is highly accurate.

This paper is organized as follows: In Section II, related works are briefly reviewed. In Section III, the models for the camera and projector are introduced. In Section IV, the proposed calibration system that makes use of an LCD panel as the calibration plane is presented. The calibration steps are also outlined. In Section V, extensive experimental results that evaluate the performance of the proposed calibration design in a number of different measures and compare it with that of the traditional methods are shown. Concluding remarks and future work are given in Section VI.

II. Previous Work

Much work has addressed camera calibration. Among the most widely used camera calibration methods are Tsai's method [8] and Zhang's method [9]. Tsai's method relies on accurate 3-D measurement with respect to an external 3-D calibration object to which a reference coordinate frame is defined. All the measurements of position and orientation are with respect to this reference coordinate frame. The method has been widely used in multicamera applications. Zhang's work adopts the use of a planar calibration object instead. The advantages of the method are that the planar calibration object is easier to construct than the 3-D calibration object, and both the extrinsic (the camera-to-world or camera-to-camera geometries) and intrinsic parameters (the internal parameters) of the cameras can be calibrated in the same system. A similar method was also proposed by Sturm and Maybank [10], where the singularities of the calibration results were discussed.

In contrast, fewer works have been devoted to the calibration of the projector-and-camera system [11]. In the paper by Sansoni *et al.* [12], a relatively simple model for the optical geometry of the projector-and-camera system is proposed, which consists of three parameters: 1) the baseline; 2) the distance of the baseline from the reference surface; and 3) the orientation of the projector with respect to the camera. The system requires the use of a specially designed calibration object—a block of parallepipedic shape. Its dimensions, which are measured by a coordinate measurement machine, must have an uncertainty that is one order of magnitude less than that of the targeted 3-D resolution at which the SLS is aimed. The SLS comprises a specially developed LCD projector with video graphics array resolution and a video camera (with a resolution of 756 $\times$ 581 pixels) equipped with a closed-circuit television manual iris zoom (with a range of 12.5–75 mm). Gray code and phase shifting codification are used for 3-D reconstruction. Their experimental results show that, at a working distance of 1500 mm, depth determination can reach a resolution of 70 μm, and the estimated accuracy can reach 0.1% of the depth range. Such figures are, however, only similar to those of the other calibration systems.

In the system proposed by Sadlo *et al.* [13], a printed checkerboard pattern is used. The calibration plane is divided into two regions. One blank region is used as the projector screen, and another is covered with a printed checkerboard pattern for camera calibration. Color markings on the four corners of the checkerboard pattern are used to ease pattern detection in the image data. With an image resolution of 1024 $\times$ 768 pixels, under the calibrated system parameters, a spherical object could be reconstructed with a maximal error of 0.5 mm.

In the system developed by Legarda-Sáenz *et al.* [14], a calibration object with a size of about 800 mm $\times$ 600 mm and 140 physical target marks that are uniformly distributed over it was used. The target marks were measured with an accuracy of 0.1 mm, and they were first used for camera calibration. Then, a series of continuous periodic patterns that contain phase information (like the phase of a sinusoidal pattern) was projected from the projector to the calibration object, which was then pictured by the camera again. The phase information in the patterns was so constructed that a one-to-one correspondence between the projector's image plane and the camera's image plane could be established. That was the main contribution of this paper. Such one-to-one mapping between the projector's image plane and the cameras' image plane was then used to interpolate the image positions of the 140 target marks in the projector's image plane, thereby allowing those target marks to be like that pictured by the projector. Such image positions of the target marks in the projector were then used for projector calibration. In their experiments, a camera with a resolution of 736 $\times$ 572 and a nominal focal length of 12 mm and an LCD projector with a resolution of 832 $\times$ 624 pixels and a nominal focal length of 50 mm were used. The calibration was conducted using 19 positions of the calibration object. At a working distance of about 750 mm, the system could reconstruct a perfect plane with a standard deviation of planarity of no more than 0.4506 mm.

A similar idea was adopted by Song and Huang [15] but extended to a concept that allows the projector to be treated as if it can "capture" image. Whereas, in [14], the image positions of 140 target marks were reconstructed in the projector's image plane, here, the image of the entire calibration plane was reconstructed in the projector. With this concept, the calibration of SLS becomes essentially the same as the calibration of traditional stereo-vision systems that consist of cameras only. In [15], a root-mean-square error of planarity ranging from 0.10 to 0.22 mm was reported.

Methods such as those in [16] and [17] that require no use of calibration object gain convenience at the expense of reconstruction accuracy. In contrast, methods that require the use of calibration object can potentially achieve higher accuracy; however, the accuracy hinges upon how accurate the metric figures of the calibration object and the markings on it are produced or measured.

All in all, we believe that the approach of using a calibrated camera to calibrate the projector, even at the expense of having

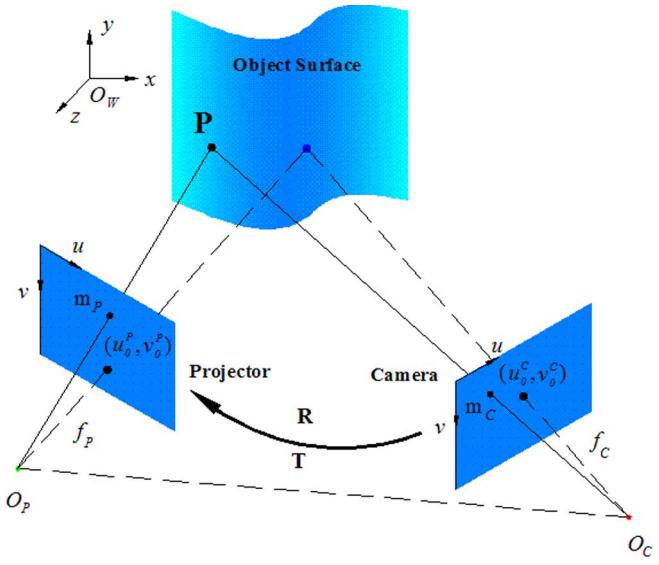

Fig.1. Geometry between the camera, projector, and the world coordinate frames. With the geometry calibrated, the depth value of any world point $\mathbf{P}$ can be calculated from the two corresponding points: (u^c, v^c) and (u^p, v^p) via triangulation.

the accuracy of projector calibration partially influenced by that of camera calibration, has simplicity and convenience and is a practical approach.

III. Projector-and-Camera System Model

The geometry between the camera, projector, and world coordinate frames is depicted in Fig. 1. The perspective pinhole model is used to model the camera and projector, as illustrated by (1) and (2).

The 3-D position $\mathbf{M}_W$ of any feature point in space, which is measured against the world coordinate frame, is related to image position $\mathbf{m}_C$ or $\mathbf{m}_P$ by the following:

$$\begin{bmatrix} \mathbf{m}_{C/P} \\ 1 \end{bmatrix} \cong \begin{bmatrix} \alpha_u^{C/P} & \gamma^{C/P} & u_0^{C/P} \\ 0 & \alpha_v^{C/P} & v_0^{C/P} \\ 0 & 0 & 1 \end{bmatrix} \begin{bmatrix} & & 0 \\ & \mathbf{I}_3 & 0 \\ & & 0 \end{bmatrix} \begin{bmatrix} \mathbf{M}_{C/P} \\ 1 \end{bmatrix} \tag{1}$$

$$\begin{bmatrix} \mathbf{M}_{C/P} \\ 1 \end{bmatrix} = \underbrace{\begin{bmatrix} \mathbf{R}_{C/P} & \mathbf{t}_{C/P} \\ 0 & 1 \end{bmatrix}}_{\mathbf{E}_{C/P}} \begin{bmatrix} \mathbf{M}_W \\ 1 \end{bmatrix} \tag{2}$$

where the notation C/P refers to either the camera and the projector measurement or parameters, with C and P pertaining to the camera and the projector, respectively. There are five intrinsic parameters (α_u^C, α_v^C, γ^C, u_0^C, and v_0^C, or α_u^P, α_v^P, γ^P, u_0^P, and v_0^P) and six extrinsic parameters [$(\mathbf{R}_C, \mathbf{t}_C)$ or $(\mathbf{R}_P, \mathbf{t}_P)$, collectively expressed as 4×4 matrix $\mathbf{E}_C$ or $\mathbf{E}_P$] for the camera and projector, respectively. With respect to the same world coordinate system, extrinsic parameters $\mathbf{E}_C$ and $\mathbf{E}_P$ can be related by matrix $\mathbf{E}$, i.e., the relative transformation matrix between the projector and camera, as indicated by (3). The calibration problem is to determine the intrinsic parameters of the camera and projector and the relative transformation matrix $\mathbf{E}$

$$\begin{bmatrix} \mathbf{M}_C \\ 1 \end{bmatrix} \cong \underbrace{\begin{bmatrix} \mathbf{R} & \mathbf{t} \\ 0 & 1 \end{bmatrix}}_{\mathbf{E}} \begin{bmatrix} \mathbf{M}_P \\ 1 \end{bmatrix}. \tag{3}$$

IV. Calibration Using LCD Panel

An accurate system model and a solution for the model parameters are important. However, another point that is often overlooked is the calibration pattern itself, particularly when high accuracy is required. Once the system model is set up, the accuracy of the system heavily relies on the pattern selection and processing. Traditionally, a printed checkerboard paper that is attached onto a planar object is used as the calibration pattern. Another distinguishable pattern projected from the projector on the same planar object is used to calibrate the projector. Often, the calibration algorithms assume that the observed plane and pattern are ideal; the print of the pattern, the manufacture of the calibration plane, and, more precisely, planarity are not considered. In reality, however, standard copy paper has a thickness variation within itself ranging from 0.08 to 0.11 mm. When this paper is attached to a planar board, the planarity of the final pattern could suffer from nonuniform folding of this paper against the board. Even the planarity of the board itself could be limited. By experience, the flatness deviation of the pattern can well exceed 0.1 mm.

To overcome these drawbacks, in this paper, we propose an alternative calibration design. We use an LCD panel as the calibration plane instead. Whereas patterns displayed on the panel are used to calibrate the camera, the patterns projected from the projector onto the panel and reflected by it at a total-dark setting of its display are used to calibrate the projector. This design has five advantages.

1) *Simple and convenient calibration setup*: A consumer LCD panel is all that is additionally required for the calibration task. Displaying the pattern in and projecting the pattern to an LCD panel are also much less tedious processes than precisely acquiring the measured pattern print and gluing it to a planar board.
2) *Ideal planarity*: The flatness of the LCD panel is of industrial grade; many off-the-shelf projectors have guaranteed that the planarity deviation of the panel is less than 0.05 μm.[1] To the stated calibration task, it is almost as if the panel surface is an ideal plane.
3) *Programmable patterns*: Different types of pattern in various combinations of colors can be generated easily by computer and displayed on the LCD panel as the calibration patterns.
4) *High accuracy*: There is no print error, and the pattern dimensions are all easily measurable in pixels of the LCD panel.
5) *High image quality*: Pattern images with high contrast can be achieved.

[1]Webpage of a major LCD panel substrate glass manufacturer: http://www.corning.com/.

A. Camera Calibration

A pattern with known dimensions on either the LCD panel in the proposed calibration setup or an external calibration board in the traditional setup is shown to the camera and imaged. Zhang's method is then adopted for camera calibration. By introducing the homography constraint between camera image plane Π_{CCD} and calibration plane Π_{LCD}, the intrinsic parameters of the camera can be estimated. Once camera intrinsic parameters $\mathbf{A}_C$ are known, the position of the camera with respect to the calibration plane or, alternatively speaking, the position of the calibration plane with respect to the camera—$(\mathbf{R}_C, \mathbf{t}_C)$—can be determined as well.

B. Projector Calibration

Once the camera is calibrated, with the spatial position and orientation of the LCD panel kept still, we employ the projector to project a known pattern onto the LCD panel. The reflection from the panel is then imaged by the camera, and the image data are used to calibrate the projector. In the process, the LCD panel is instructed to have the total-dark setting on its display, so that confusion between the displayed pattern and the reflected pattern on the calibration object in the image data—an inevitable issue in traditional calibration—is avoided. This is another advantage of using the LCD panel as the calibration object.

Suppose that we have a feature point $\mathbf{m}_p$ [i.e., (u_p, v_p)] on the projector's image plane, whose projection on calibration plane Π_{LCD} is a certain $\mathbf{P}_L$ [i.e., (x_p, y_p, z_p)]. Suppose also that $\mathbf{m}_c$ [i.e., (u_c, v_c)] is the corresponding image position on the camera's image plane that we can observe from the reflection image of Π_{LCD}. Since camera parameters $\mathbf{A}_C$ and $(\mathbf{R}_C, \mathbf{t}_C)$ have been made known from the prior camera calibration process, we have the following for $\mathbf{P}_L$:

$$\begin{bmatrix} \mathbf{m}_c \\ 1 \end{bmatrix} \cong \mathbf{A}_C \begin{bmatrix} & & 0 \\ & \mathbf{I}_3 & 0 \\ & & 0 \end{bmatrix} \begin{bmatrix} \mathbf{R}_C & \mathbf{t}_C \\ 0 & 1 \end{bmatrix} \begin{bmatrix} \mathbf{P}_L \\ 1 \end{bmatrix} \tag{4}$$

which represents two scalar constraints for $\mathbf{P}_L$. The fact that $\mathbf{P}_L$ lies on calibration plane Π_{LCD}, which has also been made known in the camera calibration process, represents the third constraint for $\mathbf{P}_L$. The three constraints together allow $\mathbf{P}_L$ to be precisely determined.

Such a correspondence between $\mathbf{m}_p$ and $\mathbf{m}_c$ represents two scalar constraints for the projector's intrinsic parameters $\mathbf{A}_P$ and extrinsic parameters $(\mathbf{R}_P, \mathbf{t}_P)$, as expressed by

$$\underbrace{\begin{bmatrix} u_p \\ v_p \\ 1 \end{bmatrix}}_{\mathbf{m}_p} \cong \underbrace{\begin{bmatrix} \alpha_u^P & \gamma^P & u_0^P \\ 0 & \alpha_v^P & v_0^P \\ 0 & 0 & 1 \end{bmatrix}}_{\mathbf{A}_P} \begin{bmatrix} & & 0 \\ & \mathbf{I}_3 & 0 \\ & & 0 \end{bmatrix} \begin{bmatrix} \mathbf{R}_P & \mathbf{t}_P \\ 0 & 1 \end{bmatrix} \underbrace{\begin{bmatrix} x_p \\ y_p \\ z_p \\ 1 \end{bmatrix}}_{\mathbf{P}_L}. \tag{5}$$

In the procedure, the 3-D information $\mathbf{P}_L$ is first determined from image data $\mathbf{m}_c$ via (4), and then, the known $\mathbf{P}_L$ is used to determine projector parameters $\mathbf{A}_P$, $\mathbf{R}_P$, and $\mathbf{t}_P$ via (5). With this, projector calibration can be treated as traditional camera calibration, which includes the determination of intrinsic and extrinsic parameters from known 3-D information. On this, any state-of-the-art camera calibration method such as those in [18]–[20] can be used to tackle the problem. Weng *et al.*'s method [19] is adopted in our work. The first step employs a noniterative algorithm to directly compute a closed-form solution of all the extrinsic parameters and some major intrinsic parameters based on a distortion-free projector model. The second step adopts a finer projector model that also incorporates lens distortion and uses the solution from the first step as an initial guess to determine all the intrinsic parameters via a nonlinear optimization process. Details of this camera calibration-like step are available in [19].

After calibration of both the camera and the projector, $(\mathbf{R}_C, \mathbf{t}_C)$ and $(\mathbf{R}_P, \mathbf{t}_P)$ can be used to determine the relative transformation matrix $\mathbf{E}$ from (3). Based on this idea, we have the calibration procedure of the projector-and-camera system modified to six steps.

1) A checkerboard pattern with known dimensions is displayed on the LCD and is imaged by the camera.
2) Keeping its position unchanged, set the LCD panel to total-dark setting, and use it as a projection screen.
3) Project a known pattern from the projector onto the LCD panel, whose reflection is again imaged by the camera. The image of the displayed pattern and that of the projected pattern form an image pair.
4) Change the pose of the LCD panel, and repeat steps 2 and 3 to acquire enough image pairs.
5) Each image pair is associated with a particular pose of the LCD panel. Use those images related to the LCD panel's pattern displays to calibrate the camera's intrinsic parameters. In addition, use the image data to determine, for each pose of the LCD panel, the position Π_{LCD} of the LCD screen with respect to the camera.
6) Then, use the image data related to the LCD panel's reflections of projected patterns to calibrate, through (4) and (5), the projector's intrinsic parameters, as well as its position with respect to the camera.

With the calibration result, depth can be recovered from the triangulation mechanism [11], as expressed by the following:

$$z_c = \frac{(\mathbf{R}\overline{\mathbf{m}}_c \cdot \overline{\mathbf{m}}_p)(\overline{\mathbf{m}}_p \cdot \mathbf{T}) - \|\overline{\mathbf{m}}_p\|^2 (\mathbf{R}\overline{\mathbf{m}}_c \cdot \mathbf{T})}{\|\mathbf{R}\overline{\mathbf{m}}_c\|^2 \|\overline{\mathbf{m}}_p\|^2 - (\mathbf{R}\overline{\mathbf{m}}_c \cdot \overline{\mathbf{m}}_p)^2} \tag{6}$$

where $\overline{\mathbf{m}}_c$ and $\overline{\mathbf{m}}_p$ refer to the two corresponding points on the camera's and projector's image planes, respectively, in homogeneous coordinates.

We have incorporated lens distortion parameters in calibrating the camera and the projector in the same way as in the calibration systems in [9] and [19] that we have adopted. However, our experiments show that the distortions in both the camera (we used a Pentax K100D digital single lens reflex (DSLR) camera with Pentax DA 18–55-mm lens, which are both only consumer-level equipment) and the projector (we used a NEC LT25 projector, which is also consumer-level equipment) were relatively small in relation to our task and imposed almost no

effect on the accuracy of the final reconstruction. For simplicity, we thus skip the use of the lens distortion parameters for 3-D reconstruction in the triangulation process.

Notice that there exist more robust triangulation methods [21], which more globally conduct 3-D determination like considering the minimization of the sum of squared differences between the corresponding points in the two images. Such methods are particularly useful in the case that a large noise is present in the image positions of the feature points. However, in our system, the feature points on the projector side are generated data and not observed data, and they are known *a priori* without much error. Our experiments show that, for the equipment with which we experimented, direct triangulation already offers a sufficiently accurate result.

In the procedure, the camera and projector use the same calibration plane but different patterns for calibration. Whereas the camera is calibrated from patterns displayed on the LCD screen, the projector is calibrated from the reflection of patterns on the screen. By using the LCD panel as the calibration plane, errors caused by imperfections of the patterns and the calibration plane, and confusion between the displayed pattern and the reflected pattern in the image data, could be much reduced.

V. Experimental Result

A. Reprojection Error

In this experiment, the calibration quality is evaluated based on the reprojection error, which is the average Euclidean distance in the image space between two sets of image positions—the observed image positions of certain image features and those that are projected to the image plane from the corresponding features in 3-D (on the calibration plane) using the calibrated camera parameters. We compared the results of our calibration design with those of the traditional setup.

The projector-and-camera system we used in our experiments consisted of a DLP projector with a resolution of 1024×768 (NEC LT25 projector) and a camera with a resolution of 2400×1600 (Pentax K100D DSLR camera with Pentax DA 18–55-mm lens), both being off-the-shelf equipment. The focal length of the camera was in the range of 18–55 mm, and that of the projector was in the range of 25–31 mm. The SLS was configured for a working distance (the distance from the camera to the mean position of the target object) of about 750 mm and an object thickness of about 50 mm (but not exceeding 100 mm).

The calibration setup comprised a 15-ft LCD panel that was used as the calibration plane. At any new pose of the LCD panel, the orientation of the LCD panel was adjusted to avoid reflection glare. The calibration patterns we used are displayed in Fig. 2. The use of the LCD panel let the calibration patterns be displayed with high contrast, allowing the pattern image to be processed with ease and accuracy. We had tried as many as 20 images (under different positions and orientations of the LCD panel) for camera calibration, but the result showed that six to eight images were generally enough to obtain stable calibration parameters. We therefore used only eight images for calibration in all the experiments. In contrast, experiments

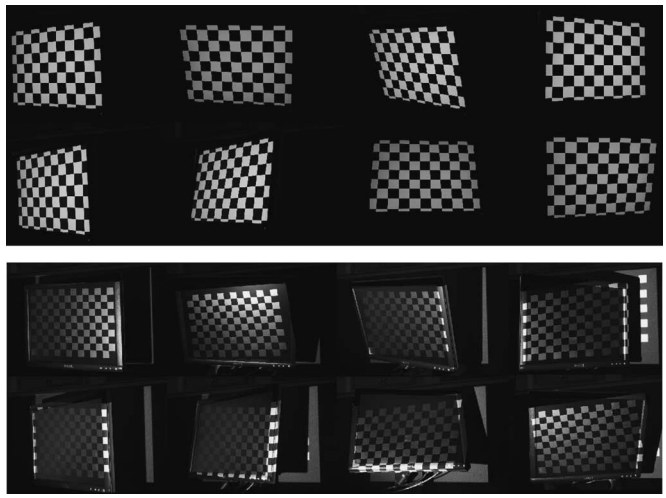

Fig. 2. (Top) Checkerboard pattern displayed on the LCD screen for camera calibration in our setup. (Bottom) Patterns projected onto the LCD screen for projector calibration.

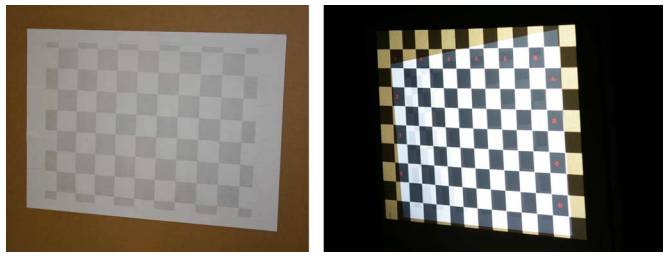

Fig. 3. (Left) Checkerboard pattern print with a gray level of 128 that was for camera calibration under the traditional calibration design. (Right) Reflected pattern on top of the pattern print that was for projector calibration.

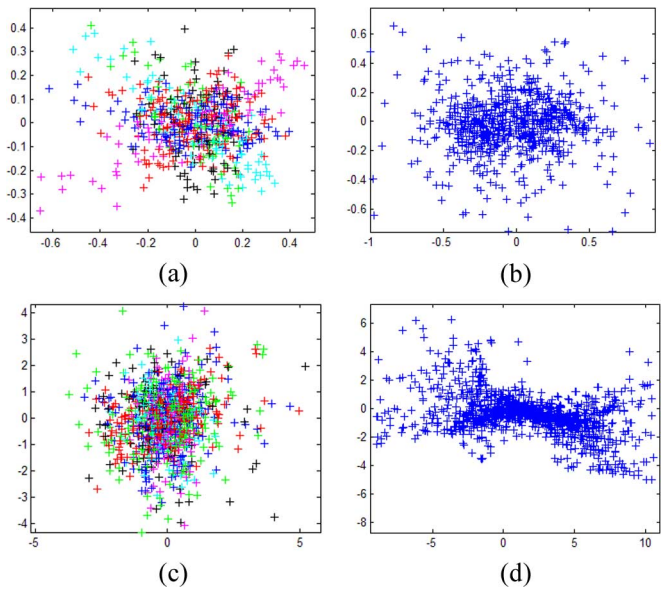

Fig. 4. Reprojection error distribution. (a) Camera calibration result and (b) projector calibration result, both from the use of the LCD panel as the calibration object. (c) Camera calibration result and (d) projector calibration result, both from the use of the printed pattern as the calibration object.

show that the traditional method required 20–30 images to have enough calibration accuracy on the same projector-and-camera system. We believe the great reduction in the required image

TABLE I
CALIBRATION RESULTS FROM THE USE OF LCD PANEL AND PRINTED PATTERN, RESPECTIVELY (IN PIXELS)

Parameter	*LCD Pattern*	*Printed pattern*
Camera RPE	[0.1308 0.0994]	[1.0446 1.3258]
f_C	[3255.9 3265.5] ± [3.9 3.5]	[3204.6 3197.8] ± [24.3 23.6]
u_{C0}, v_{C0}	[1199.8 835.0] ± [3.6 2.9]	[1380.4 837.5] ± [45.8 30.3]
Projector RPE	[0.4720 0.3281]	[6.1614 3.2826]
f_P	[2225.6 2223.8] ± [12.6 12.5]	[1962.3 1876.7] ± [47.1 45.1]
u_{P0}, v_{P0}	[511.7 747.8] ± [5.8 16.5]	[686.4 698.9] ± [78.4 98.8]

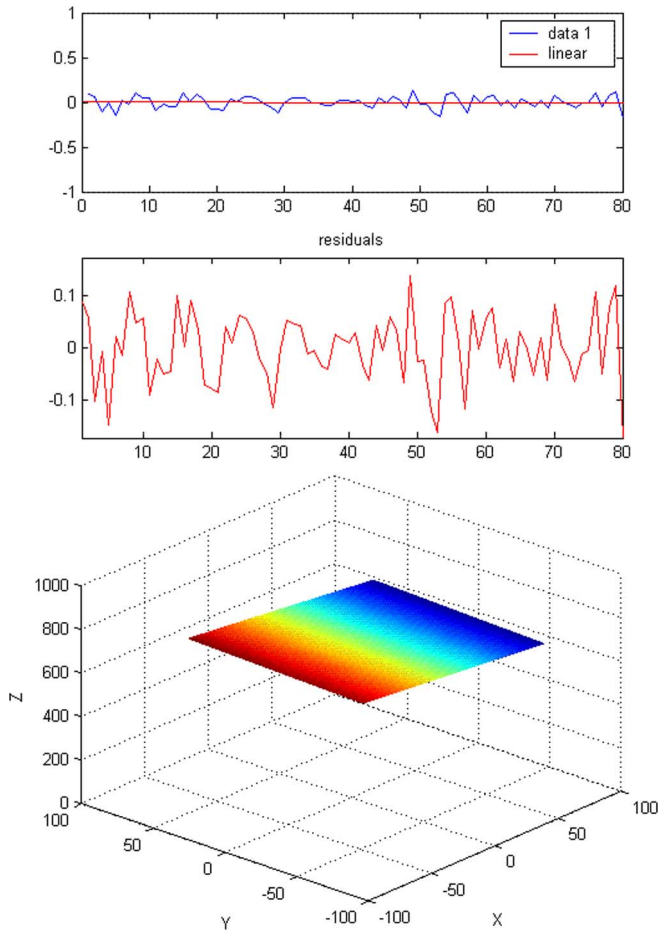

Fig. 5. (Top) Residual errors with respect to the fitted plane under the proposed calibration setup. (Bottom) Reconstruction of the plane with respect to the camera coordinate frame. The reconstructed plane had an orientation $[-0.4611, 0.0259, -0.8870]$ with respect to the camera reference frame.

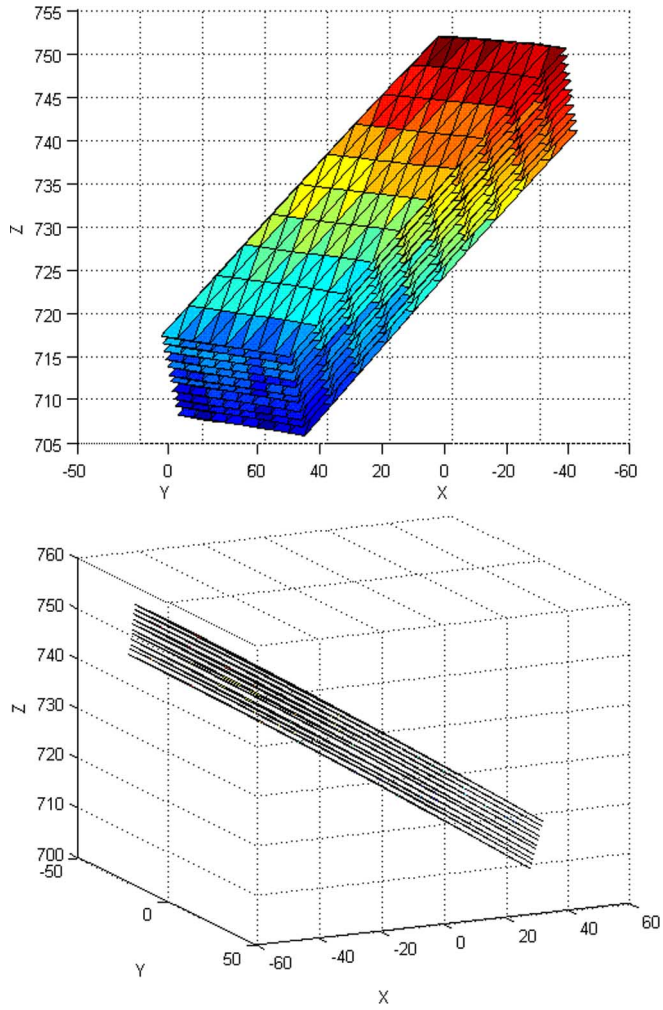

Fig. 6. (Top) Eleven reconstructed planes under the proposed calibration. (Bottom) Side view of the reconstructed planes.

number is due to the many advantages of using the LCD panel as the calibration object.

The traditional calibration setup we employed in our experiments used a printed checkerboard pattern of A4 size as the calibration object. In traditional calibration setup, there is always the issue of confusion between the pattern print and the reflected pattern in the image data. We avoided confusion by having the pattern print purposefully made of a rather light gray level—a gray level of 128. As shown in Fig. 3, this allowed the pattern print and the reflected pattern to be more distinguishable. In the experiments with the traditional calibration setup, a total of 20 pairs of images under different poses of the calibration object were used.

Following the procedure described in Section IV, the system was calibrated with our calibration setup and the traditional calibration setup, respectively. The reprojection error distributions of the camera and the projector are shown in Fig. 4. Some major calibration parameters are listed in Table I: *RPE* is the reprojection error; f_C and f_P are the focal lengths; and (u_{C0}, v_{C0}) and (u_{P0}, v_{P0}) are approximately the principal points of the camera and the projector, respectively. The skew parameter and aspect ratio of both equipment were very close to 0 and 1, so we did not include them in Table I. The result shows that, with the use of the LCD panel, uncertainty can be reduced by five to ten times, with even less than half of the images used (eight versus 20). The *RPE* was about 0.1 pixels only under the use of eight calibration images in the proposed calibration design. The *RPE* in projector calibration can be controlled to within 0.5 pixels. Compared with the *RPE* of six pixels in the use of

TABLE II
MEASUREMENT RESULTS OF THE VARIOUS MOTION STEPS OF A MOVING PLANE (IN MILLIMETERS)

	1	*2*	*3*	*4*	*5*	*6*	*7*	*8*	*9*	*10*	*Mean*
Proposed Calibration	0.986	0.986	1.060	0.942	1.128	0.851	1.076	1.074	0.876	1.075	1.005
Traditional Calibration	1.102	1.112	1.174	1.063	1.249	0.846	1.316	1.191	0.939	1.265	1.126

the printed calibration pattern, the improvement was more than ten times.

Fig. 4(d) shows a certain nonuniformity in the distribution, but the nonuniformity does not always show up in the experiments the we have conducted, and when it shows up, it does not appear to have any particular pattern. We believe that the occasional nonuniformity of the distribution comes from the uneven nonplanarity of the printed pattern and board, and features chosen from different parts of the calibration object cause different error distributions.

B. Planarity Check

In this experiment, we directly evaluate the improvement in 3-D reconstruction under the proposed calibration design, as 3-D reconstruction is the ultimate goal of the system. We compared the measured planarity of an ideal plane using the calibration parameters obtained from our calibration system and from the traditional one (which used a printed pattern as the calibration object). We chose the LCD panel itself as the ideal plane, as its planarity is of an assured quality close enough to ideality. It was placed about 750 mm away from the camera in all related experiments.

In both calibration systems, a pattern was projected onto the LCD panel surface, some feature points were extracted, and their depth values were calculated with the calibration parameters. A total of 80 points were extracted, and their depth values were calculated through triangulation with respect to the camera reference frame. A plane was then fitted to the reconstructed 3-D points.

With calibration result from the proposed calibration system, the residual errors of the points with respect to the aforementioned "fitted" plane were calculated and plotted in Fig. 5. The error had a root-mean-square value of 0.04 mm and a standard deviation of 0.05 mm. When the calibration result obtained from the printed calibration pattern was used for 3-D determination, the error had a root-mean-square value of 0.405 mm and a standard deviation of 0.480 mm. The result shows that 3-D reconstruction accuracy can be improved by almost ten times under the new calibration system.

C. Motion Measurement

In this experiment, the known motion of a plane is used to evaluate the calibration accuracy. A linear stage with a motion accuracy of 1 μm was used to move an external plane. The plane was shifted ten times, in steps of 1 mm. After each motion, a pattern was projected on the plane for its reconstruction. A total of 11 planes were reconstructed, and the results under the proposed calibration are shown in Fig. 6. The distances between every two adjacent planes were calculated, and they are shown in Table II. The mean value of the measurement under the proposed calibration setup had an error standard deviation of 5 μm or 0.001% of the depth range, whereas that under the traditional calibration setup had an error standard deviation of 0.126 mm. That was an accuracy improvement of 25 times.

VI. CONCLUSION AND FUTURE WORK

We have described an accurate, convenient, and efficient method for projector-and-camera system calibration. The calibration system makes use of an LCD panel as the calibration plane. In our experiments, a reprojection error of 0.1 pixel was achieved in the camera calibration using only eight images, which shows that uncertainty and reprojection error could be much reduced. The root-mean-square error in the planarity check was found to be only 0.04 mm, and a mean deviation of only 5 μm or 0.001% of the depth range was obtained when measuring a motion distance of 1 mm. Both indicate significant improvement over those of the traditional calibration setup. The result shows that, by using the LCD panel as the calibration plane, the projector-and-camera system parameters can be calibrated in far fewer images with much higher accuracy. In fact, the programmability of the LCD panel in its pattern display makes the system more adaptable to other tasks and opens up many other applications. Future work will address how the calibration setup can be extended for a projector-and-camera system that consists of multiple cameras.

ACKNOWLEDGMENT

This work is affiliated with the Microsoft-CUHK Joint Laboratory for Human-centric Computing and Interface Technologies.

REFERENCES

[1] J. Salvi, J. Pagès, and J. Batlle, "Pattern codification strategies in structured light systems," *Pattern Recognit.*, vol. 37, no. 4, pp. 827–849, 2004.
[2] R. Zhang, P. Tsai, J. E. Cryer, and M. Shah, "Shape from shading: A survey," *IEEE Trans. Pattern Anal. Mach. Intell.*, vol. 21, no. 8, pp. 690–706, Aug. 1999.
[3] S. K. Nayar, M. Watanabe, and M. Noguchi, "Real-time focus range sensor," *IEEE Trans. Pattern Anal. Mach. Intell.*, vol. 18, no. 12, pp. 1186–1198, Dec. 1996.
[4] S. Inokuchi, K. Sato, and F. Matsuda, "Range imaging system for 3-D object recognition," in *Proc. Int. Conf. Pattern Recog.*, 1984, pp. 806–808.
[5] D. Bergmann, "New approach for automatic surface reconstruction with coded light," in *Proc. SPIE—Remote Sensing Reconstruction Three-Dimensional Objects Scenes*, 1995, vol. 2572, pp. 2–9.
[6] E. M. Petriu and T. Bieseman, "Visual object recognition using pseudo-random grid encoding," in *Proc. IEEE/RSJ Int. Conf. Intell. Robots Syst.*, 1992, pp. 1617–1624.
[7] E. Horn and N. Kiryati, "Toward optimal structured light patterns," *Image Vis. Comput.*, vol. 17, no. 2, pp. 87–97, 1999.
[8] R. Y. Tsai, "A versatile camera calibration technique for high accuracy 3D machine vision metrology using off-the-shelf TV cameras and lenses," *IEEE J. Robot. Autom.*, vol. RA-3, no. 4, pp. 323–344, Aug. 1987.
[9] Z. Zhang, "A flexible new technique for camera calibration," *IEEE Trans. Pattern Anal. Mach. Intell.*, vol. 22, no. 11, pp. 1330–1334, Nov. 2000.

[10] P. Sturm and S. Maybank, "On plane-based camera calibration: A general algorithm, singularities, applications," in *Proc. IEEE CVPR*, 1999, pp. 432–437.
[11] M. Ribo and M. Brandner, "State of the art on vision-based structured light systems for 3D measurements," in *Proc. IEEE Int. Workshop Robot. Sens. Environ.*, Ottawa, ON, Canada, 2005, pp. 2–6.
[12] G. Sansoni, M. Carocci, and R. Rodella, "Calibration and performance evaluation of a 3-D imaging sensor based on the projection of structured light," *IEEE Trans. Instrum. Meas.*, vol. 49, no. 3, pp. 628–636, Jun. 2000.
[13] F. Sadlo and T. Weyrich *et al.*, "A practical structured light acquisition system for point-based geometry and texture," in *Proc. Eurographics Symp. Point-Based Graph.*, 2005, pp. 89–98.
[14] R. Legarda-Sáenz, T. Bothe, and W. P. Jüptner, "Accurate procedure for the calibration of a structured light system," *Opt. Eng.*, vol. 43, no. 2, pp. 464–471, 2004.
[15] S. Zhang and P. S. Huang, "Novel method for structured light system calibration," *Opt. Eng.*, vol. 45, no. 8, p. 083 601, 2006.
[16] D. Fofia, J. Salvib, and E. M. Mouaddib, "Uncalibrated reconstruction: An adaptation to structured light vision," *Pattern Recognit.*, vol. 36, no. 7, pp. 1631–1644, 2003.
[17] Y. F. Li and S. Y. Chen, "Automatic recalibration of an active structured light vision system," *IEEE Trans. Robot. Autom.*, vol. 19, no. 2, pp. 259–268, Apr. 2003.
[18] R. K. Lenz and R. Y. Tsai, "Techniques for calibration of the scale factor and image center for high accuracy 3-D machine vision metrology," *IEEE Trans. Pattern Anal. Mach. Intell.*, vol. 10, no. 5, pp. 713–720, Sep. 1988.
[19] J. Weng, P. Cohen, and M. Herniou, "Camera calibration with distortion models and accuracy evaluation," *IEEE Trans. Pattern Anal. Mach. Intell.*, vol. 14, no. 10, pp. 965–980, Oct. 1992.
[20] J. Heikkil and O. Silvén, "A four-step camera calibration procedure with implicit image correction," in *Proc. IEEE Comput. Soc. Conf. Comput. Vis. Pattern Recog.*, 1997, pp. 1106–1112.
[21] R. Hartley and A. Zisserman, *Multiple View Geometry in Computer Vision*, 2nd ed. Cambridge, U.K.: Cambridge Univ. Press, 2004.

Zhan Song was born in Shandong, China, in 1978. He received the M.S. degree in mechanical engineering from Dalian University of Technology, Dalian, China, in 2003. He is currently working toward the Ph.D. degree with the Department of Mechanical and Automation Engineering, the Chinese University of Hong Kong.

His current research interests include structured light systems, image processing, and 3-D face recognition.

Ronald Chung (SM'99) received the B.S.E.E. degree from the University of Hong Kong, Hong Kong, and the Ph.D. degree in computer engineering from the University of Southern California, Los Angeles.

He had been an Integrated Circuit Design Engineer and an Electronics Engineer in industry. He is currently with the Chinese University of Hong Kong as Director of the Computer Vision Laboratory and a Professor with the Department of Mechanical and Automation Engineering. His research interests include computer vision and robotics.

Prof. Chung is a member of MENSA. He was the Chairman of the IEEE Hong Kong Section Joint Chapter of the Robotics and Automation and Control Systems Societies from 2001 to 2003.